Use of the Pocket G-PFEM to Predict Changes in Soil State

Jessé J.V. Carneiro[1#], *Guilherme* H. S. Pinto[1], *André* O. Faria[1], and *Mauro* P. S. Junior[1]

[1]*Pimenta de Ávila Consultoria, Geotechnical Engineering, Alameda Oscar Niemeyer, 420 - Sereno Valley, Nova Lima, Brazil*

[#] *Corresponding author: jesse.carneiro@pimentadeavila.com.br*

ABSTRACT

Simulating the CPTu response to changes in the current soil state allows geotechnical engineers to evaluate different scenarios and better predict the structure's performance. Developed by the Universitat Politècnica de Catalunya, Centre Internacional de Mètodes Numèrics en Enginyeria and TU Graz, the Pocket G-PFEM is a numerical tool that simulates the CPTu in a homogeneous soil layer, adopting an updated Lagrangian description. Two types of cones can be simulated: i) the smooth cone, without lateral friction in the interface cone/soil, and ii) the rough cone, with lateral friction. The Clay and Sand Model is adopted as the soil constitutive model. This study assessed the software response to changes in the overconsolidation ratio (OCR) and compressibility parameters (λ and κ) in both cone modules. The rough cone analyses resulted in higher q_t and u_1 than the smooth cone, but no significant change was observed in u_2 and u_3. The Pocket G-PFEM could partially reproduce the expected behaviours from the literature, but u_2 and u_3 did not decrease significantly for high OCRs, and the rough cone could not adequately simulate the f_s. Following the literature, q_t was mainly sensitive to λ for the OCR = 1 and to κ for the OCR = 2, but an unexpected behaviour was observed for the OCR = 8 when changing λ and κ. The results show Pocket G-PFEM's limitation in reproducing q_t, f_s, and u for high OCRs. It might be related to the adopted parameters, and different sets should be evaluated.

Keywords: Numerical tool; CPTu; OCR; compressibility parameters.

1. Introduction

The Cone Penetration Test with porewater pressure measurement (CPTu) gives the soil's mechanical response and pore pressure profiles at the moment of the test. However, changes in the boundary conditions, such as water level fluctuations, stress relief (e.g., due to an excavation), or stress increase (e.g., due to the construction of a new embankment), can considerably affect the soil behaviour and its parameters. Numerical reproduction of the CPTu allows engineers to predict the different outcomes of geotechnical interventions in a soil layer by simulating the changes in boundary conditions.

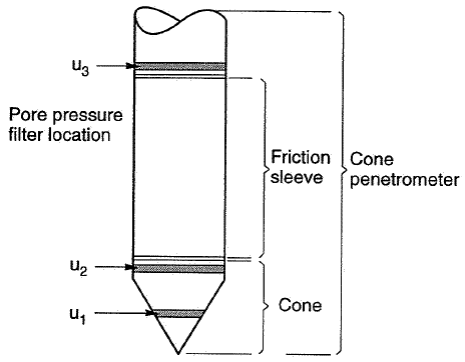

Figure 1. Typical cone design (adapted from Lunne *et al.* 1997).

Considering the international standard 22476-1 (ISO 2022), the CPTu consists of a cone with 10 cm² to 15 cm² area pushed at 2.0 ± 0.5 cm/s with readings taken every 2 cm or 5 cm. A typical cone is presented in Figure 1, where are taken five independent measurements:

- The cone tip resistance (q_c), which characterizes the soil resistance to the cone penetration;
- The sleeve friction (fs), which is the measurement of the soil adhesion on the friction sleeve and
- The porewater pressure at different positions: u_1 - at the cone tip, u_2 - at the cone shoulder, and u_3 - behind the sleeve.

The measured cone tip resistance (q_c) needs to be corrected to total cone resistance (q_t) by Eq. (1), where a is the net area ratio, around 0.80, to contemplate the porewater pressure effect in unequal areas (Lunne *et al.*, 1997).

$$q_t = q_c + u_2(1 - a) \quad (1)$$

Mayne (2001) demonstrated that the porewater pressure measured by the cone comprises three parcels, as shown in Eq. (2).

$$u = u_o + \Delta u_{oct} + \Delta u_{shear} \quad (2)$$

Whereas u_0 is the equilibrium porewater pressure existing before the cone penetration, Δu_{oct} is the octahedral component of excess porewater pressure, and Δu_{shear} is the shear component of excess porewater pressure. As detailed by the author, the octahedral component is always positive, and the shear-induced parcel can be positive or negative depending on the material condition (normally or overconsolidated).

1.1. Influence of overconsolidation

According to Robertson *et al.* (1986) and Roy *et al.* (1982), in a saturated soil layer, porewater pressures measured on the face of the cone (u_1 position) result from

both large shear and normal stresses while the porewater pressures measured immediately behind the tip (u_2 position) result mainly from high shear stresses. Consequently, the porewater pressures measured on the cone shoulder are more representative of the induced shear behaviour. Fig. 2 compares the porewater pressure generated in the three piezo sensor locations (u_1, u_2 and u_3) of soils with different overconsolidation and stiffness, ranging from soft normally consolidated (OCR = 1) to stiff heavily overconsolidated soils (OCR = 20). The more overconsolidated the soil, the higher the porewater pressure registered at the cone tip due to the significant increase in the normal stresses during the cone penetration, whereas stress relief tends to occur in the cone sleeve, resulting in a porewater pressure decrease (at u_2 and u_3 positions).

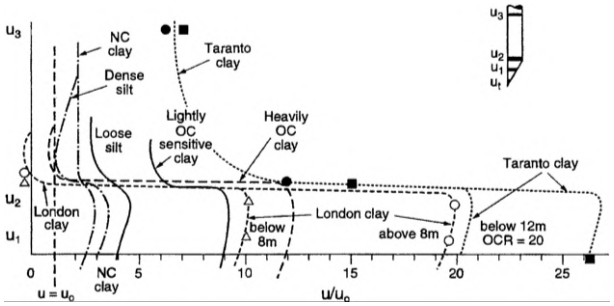

Figure 2. Porewater pressure generation at different positions to different soils (Robertson, *et al.* 1986).

Song *et al.* (2019) performed numerical simulations using the Modified Cam Clay model (MCC) to evaluate the effect of overconsolidation in the porewater pressure generation during the cone penetration. Fig. 3 shows one of the results obtained by the authors, in which the highest OCR resulted in the highest porewater pressure at the u_1 position, similar to what was observed experimentally by Robertson *et al.* (1986).

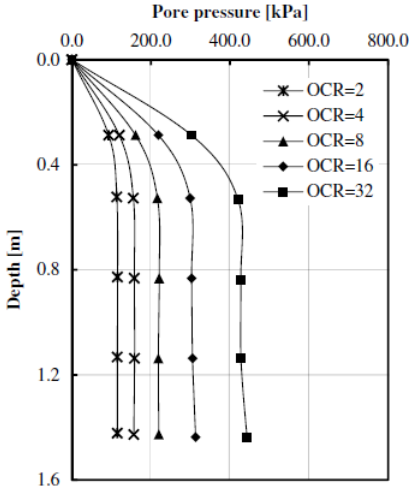

Figure 3. Variation porewater pressure profile in the cone face, u_1 position (Song, *et al.* 2019).

In Fig. 4, Song *et al.* (2019) evaluated the variation of total mean stress (p), the deviator stress (q) and the porewater pressure (u) at a fixed point in the middle of the layer (depth = 0.45 m) adjacent to the cone, in two different conditions (OCR = 2 and OCR = 32). In both scenarios, a positive excess porewater pressure peak occurs when the cone reaches the depth of 0.45 m, followed by a rapid porewater pressure relief after the tip passes it. The porewater pressure remains positive with OCR = 2, but it becomes negative with OCR = 32. The mean stress follows the porewater pressure profile, while the deviatoric stress remains constant after the cone passes the point.

As described by the authors, after the cone reaches the fixed point in a normally consolidated/lightly overconsolidated soil (in this case, OCR = 2), p is greater than q, and the porewater pressure is predominately generated by the induced normal stress, being positive, as observed in Fig. 4a. However, in highly overconsolidated soils (in this case, OCR = 32), q is greater than p, and the porewater pressure (u) is predominantly generated by the induced shear stress, being negative, as observed in Fig. 4b.

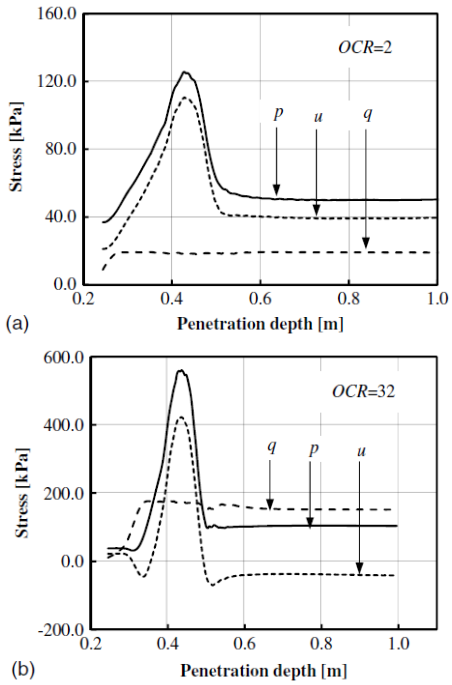

Figure 4. Variation of total mean stress (p), deviator stress (q), and porewater pressure (u) at 0.45 m deep: a) OCR equal to 2; and b) OCR equal to 32 (Song, *et al.* 2019).

1.2. Influence of compressibility

The soil compressibility also affects the cone tip resistance. As detailed by Robertson & Campanella (1983), Jamiolkowski *et al.* (1985), Lunne *et al.* (1997), Robertson (2009), Jefferies & Been (2016), in the same state condition, more compressible soils tend to present lower cone tip resistance (Fig. 5). In this way, considering numerical simulations using MCC model, it is expected that variations in the normal compression line slope (λ) and the recompression/expansion line slope (κ) affect the cone tip resistance.

This paper compares the results of the Pocket G-PFEM (CIMNE, 2023) and the expected results of the cone penetration test based on a literature review. Two main aspects were evaluated: (i) the effect of the OCR in q_t, f_s, u_1, u_2 and u_3, and (ii) the soil compressibility (by changing λ and κ) in q_t. By testing different scenarios, it

was possible to evaluate the results of the smooth and rough cone modules of the applied software.

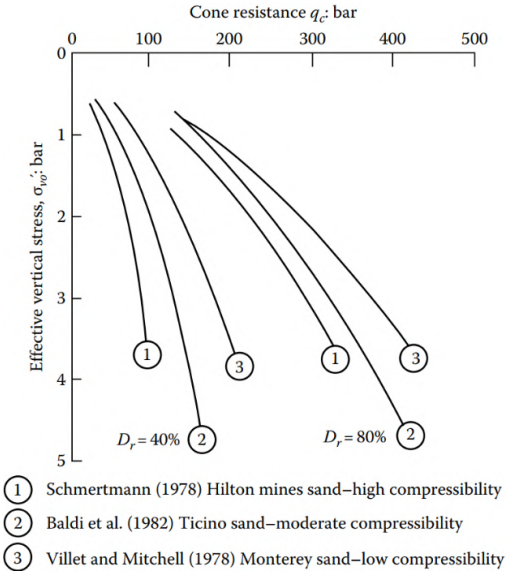

Figure 5. Comparison of the CPTu resistance of three sands with different compressibility (Robertson & Campanella, 1983).

2. Pocket G-PFEM

The application G-PFEM (Geotechnical Particle Finite Element Method) is an implementation of the Particle Finite Element Method (PFEM) within the Kratos Multiphysics framework and was primarily developed at Universitat Politècnica de Catalunya (UPC), Centre Internacional de Mètodes Numèrics en Enginyeria (CIMNE), and TU Graz. It utilizes an Updated Lagrangian description, solving governing equations with numerical techniques akin to the classical Finite Element Method (FEM), making it compatible with FEM developments. PFEM's integration domain involves a dynamic particle cloud serving as nodes in the finite element mesh, featuring h-adaptivity for refinement in regions with significant deformations (CIMNE 2023).

The CPTu is simulated as an axisymmetric problem in a homogeneous profile of 1.0 m deep and 0.7 m wide. The frictional contact between the cone (rigid body) and the soil layer (deformable domain) obeys a Coulomb friction law with a contact friction angle of 10° and a penalty method to treat solution constraints with a tangential ratio of 0.01 (CIMNE 2023, Hauser and Schweiger 2021). Two modules are available: (i) the smooth cone, which only accounts for perpendicular forces to the cone surface, so no friction between the cone lateral surface and the soil is considered (no sleeve friction measurements), and (ii) the rough cone, which also accounts for parallel forces to the cone surface, so it considers the friction between the cone lateral surface and the soil.

Both modules have a predefined 10 cm² cone simulated as a rigid body, with the tip starting at the coordinates (0.0, 0.0). The numerical domain extends in depth from (0.0, 0.2) to (0.0, -0.8). Thus, the cone starts already embedded in the soil to avoid an initial situation in which the cone tip is in contact with one node, resultant of the insertion of the cone in the soil. Moreover, the numerical simulation stops at the coordinates (0.0, -0.5) to avoid any boundary effects at the end of the analysis.

To simulate a constant stress field, both water and soil are adopted weightless, and the initial stress is defined by inputting the overburden stress (σ_v) and initial porewater pressure (u_0). Deformation is constrained in the edges of the domain and impervious boundary conditions are adopted to its left and right extremities, allowing vertical deformation in y axis and making deformations impossible in both directions in the x direction. Fig. 6 shows the boundary conditions applied.

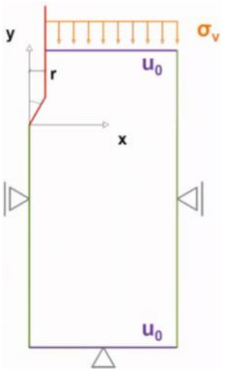

Figure 6. Pocket G-PFEM model setup and boundary conditions (CIMNE, 2023).

3. Clay And Sand Model (CASM)

The software adopts the Clay and Sand Model (CASM) as the constitutive model for the soil. Yu (1998) introduced the CASM as a unified critical state constitutive model designed in terms of a state parameter for both clay and sand under both drained and undrained loading conditions. Yu (1998) modified the yield function of the original Cam-Clay model, introducing flexibility through two additional parameters: the shape parameter (n) and the spacing ratio (r). This adjustment aimed to enhance the reproduction of peak conditions in both drained (dense soils) and undrained conditions (loose soils).

The adoption of suitable values for n and r allowed CASM to represent both bullet and elliptical shapes observed in the original Cam-Clay (n = 1 and r = 2.718) and the Modified Cam-Clay (n = 1.5 and r = 2). Furthermore, from its inception, CASM incorporated a non-associated flow rule, so the plastic potential does not mirror the shape of the yield surface, which is described according to Eq. (3).

$$f = \left(\frac{q}{M_\theta p'}\right)^n + \frac{\ln\left(p'/p_0'\right)}{\ln r} \tag{3}$$

Where, p' and q are the effective stress invariants, M_θ is the critical state stress ratio, dependent on the Lode angle, and p'_0 is the initial preconsolidation effective stress.

Pocket G-PFEM adopts the alternative potential function (g) with the introduction of the m parameter proposed by Mánica *et al.* (2022), according to Eq. (4).

$$g = \left(\frac{q}{M_\theta p'}\right)^m + m - \frac{p_0'(m-1)}{p'} - 1 \tag{4}$$

Where, *m* controls the shape of the plastic potential function (m = 2 gives a plastic potential similar to the Modified Cam-Clay yield surface).

4. Methodology

Table 1. Parameter adopted in the CPTu simulation.

Parameter	Value adopted
Initial vertical effective stress	16 kPa
Initial horizontal effective stress	16 kPa
Earth pressure coefficient (K_0)	1.0
Initial porewater pressure	0 kPa
Effective Friction angle	30º
Isotropic compression slope (λ)	0.05/0.10/ 0.15
Swelling slope (κ)	0.01/0.02/ 0.03
OCR	1/2/8/16/32
Initial porosity	0.50
Permeability	10^{-11} m/s
Poisson	0.30
Shape of the yield surface (n)	1.5
Spacing ratio (r)	2.0
Shape of the plastic potential (m)	2.0

This study adopted an isotropic model to test the Pocket G-PFEM. The soil layer was designed with a mean effective stress of 16 kPa (p' = 16 kPa), and the OCRs were simulated by adjusting the pre-consolidation stresses to 16, 32, 128, 256, 512 kPa (OCR = 1, 2, 8, 16 and 32, respectively).

The constitutive model parameters presented by Song *et al.* (2019) were adopted in the analyses. Thus, in the yield function, n was adopted equal to 1.5, r = 2, and m was adopted equal to 2 in the plastic potential to reproduce a similar behaviour to the Modified Cam-Clay (MCC) with CASM.

The compressibility effect on the CPTu results was evaluated by changing the pair λ and κ for the OCR equal to 1, 2 and 8. Nine combinations of λ (0.05, 0.10 and 0.15) and κ (0.01, 0.02 and 0.03) were simulated for each OCR. All scenarios were tested with the smooth and rough cone modules to evaluate their differences. Table 1 summarizes the initial parameter used in the CPTu modelling (base case).

5. Results

5.1. Influence of overconsolidation

Fig. 7 presents the results of the analyses to evaluate the OCR effect. It is observed that q_t, u_1 and u_2 increase with the OCR in the rough and smooth cone modules. In the rough cone, the f_s profile has a peak between 0.0 and 0.20 m, which is proportional to the OCR. Nevertheless, after 0.20 m, the values tend to zero independently of the OCR. The porewater pressure profile u_3 is near zero until 0.15 m, when it reaches a peak of negative porewater pressure. After that, the porewater pressure increases proportionally to the OCR.

The magnitude of the porewater pressure decreases with the position $u_1 > u_2 > u_3$, as stated by Robertson *et al.* (1986), but in all three positions, it is observed an increase in the porewater pressure response with the OCR increase. Nonetheless, the porewater pressure measured behind the cone tip (u_2 and u_3) in heavily overconsolidated soils should be near zero or negative, according to Lunne *et al.* (1997).

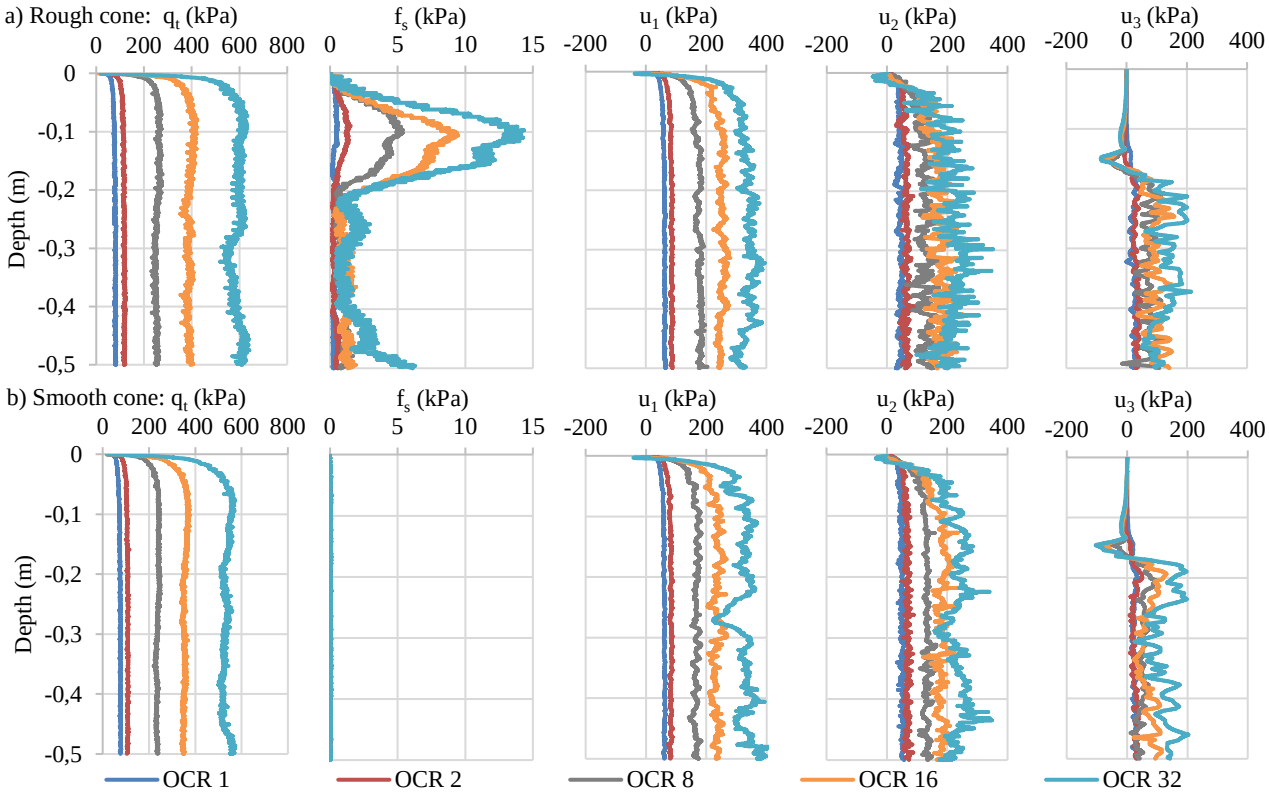

Figure 7. Results of CPTu parameters with OCR increase: a) Rough cone ($f_s \neq 0$); and b) Smooth cone ($f_s = 0$).

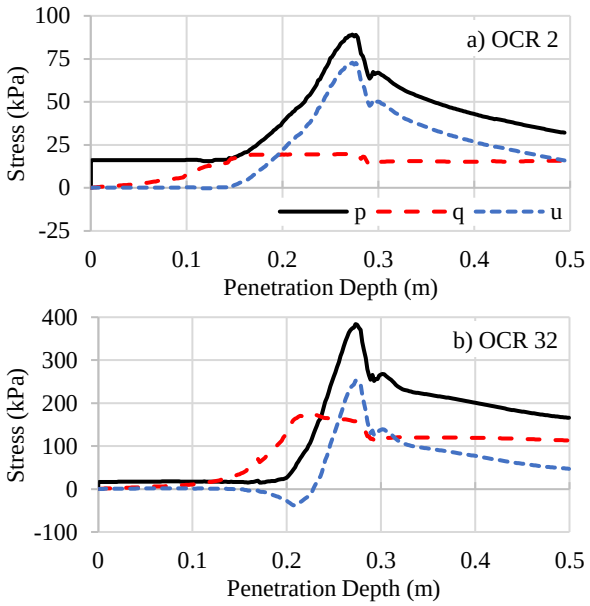

Figure 8. Variation of total mean stress (p), deviator stress (q), and porewater pressure (u) at 0.25 m deep: a) OCR equal to 2; and b) OCR equal to 32.

Since the rough cone considers the friction between the cone lateral surface and the soil, it was expected to see some difference between the u_2 and u_3 measured in the rough and smooth cone modules. However, no significant change was observed because the rough cone did not reproduce adequately the friction in the interface cone/soil. Like the q_t profile, it was expected that the *fs* profile kept constant after reaching peak values between 0.05 m and 0.20 m deep since the soil layer is homogenous. Nevertheless, as previously mentioned, it peaks and drops to almost zero, resulting in quite similar values of u_2 and u_3.

The results of the smooth and rough cones follow the same patterns. Compared to the rough cone, the magnitude of the smooth cone results is slightly lower. Like in the rough cone, the smooth cone q_t, u_1 and u_2 increase with the OCR, and u_3 is near zero until 0.15, when it peaks to a negative porewater pressure and starts to become positive, increasing proportionally to the OCR. The fs profile is the most expressive difference, which is equal to zero in the simulation, as it does not account for parallel forces to the cone surface.

Compared to the results presented by Song *et al.* (2019), u_1 has the same magnitude for all OCRs (Fig. 3 and Fig. 7). When analyzing the total stresses evolution at a point adjacent to the cone in the middle of the layer (0.02, -0.25) for OCR = 2 and OCR = 32, Fig. 8, the results for the OCR = 2 are also very similar to the ones presented by Song *et al.* (2019) in Fig. 4, but a different response is observed for OCR = 32.

In Fig. 8, it is noticeable that the total stresses start to increase earlier for the OCR = 2 than for the OCR = 32 and, after the cone passes the point, p > u > q, as presented in Fig. 4. For the OCR = 32, right before the cone reach the point, the induced porewater pressure becomes negative and rapidly increases to its maximum, like in Fig. 4. However, differently of the results presented by Song *et al.* (2019) in Fig. 4, after passing the analyzed point for the OCR = 32, the cone does not

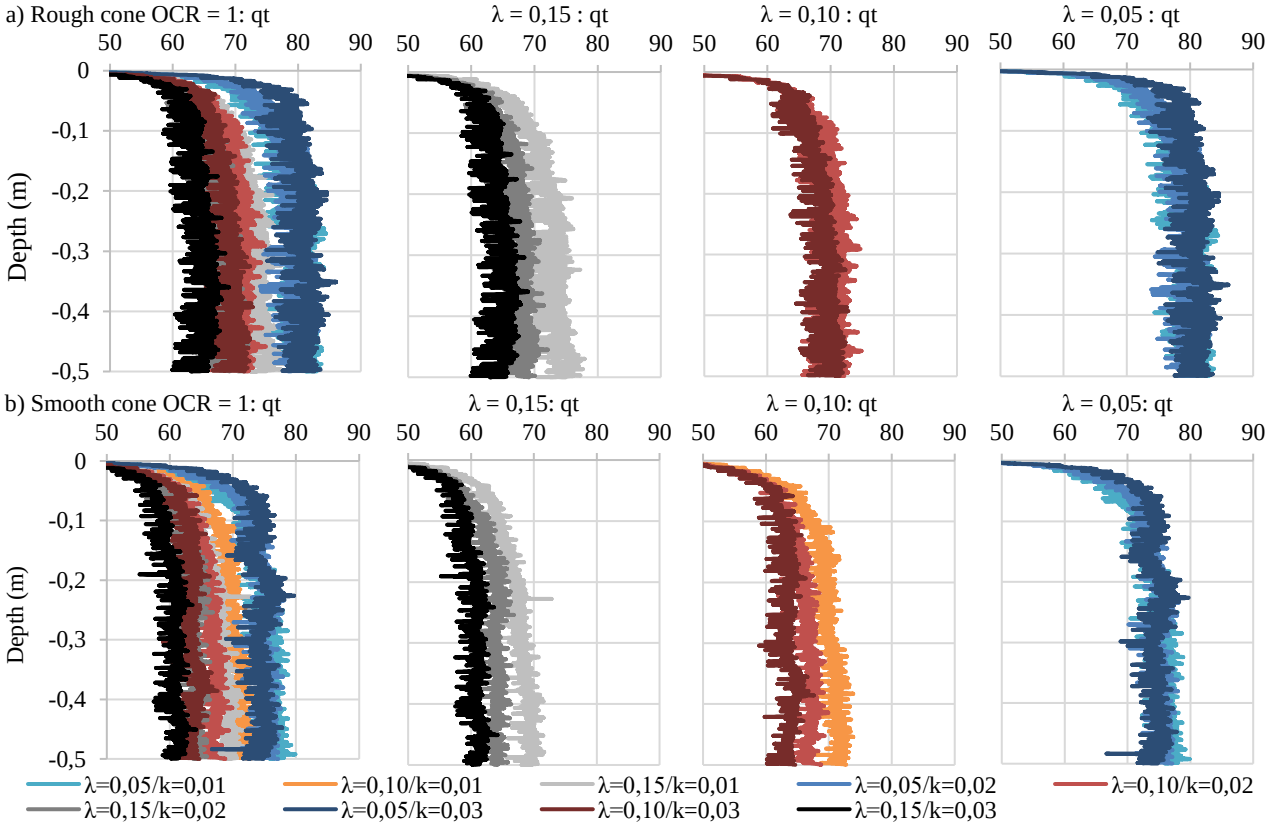

Figure 9. The influence of the compressibility parameters λ and κ in the tip resistance (q_t) for the OCR = 1.

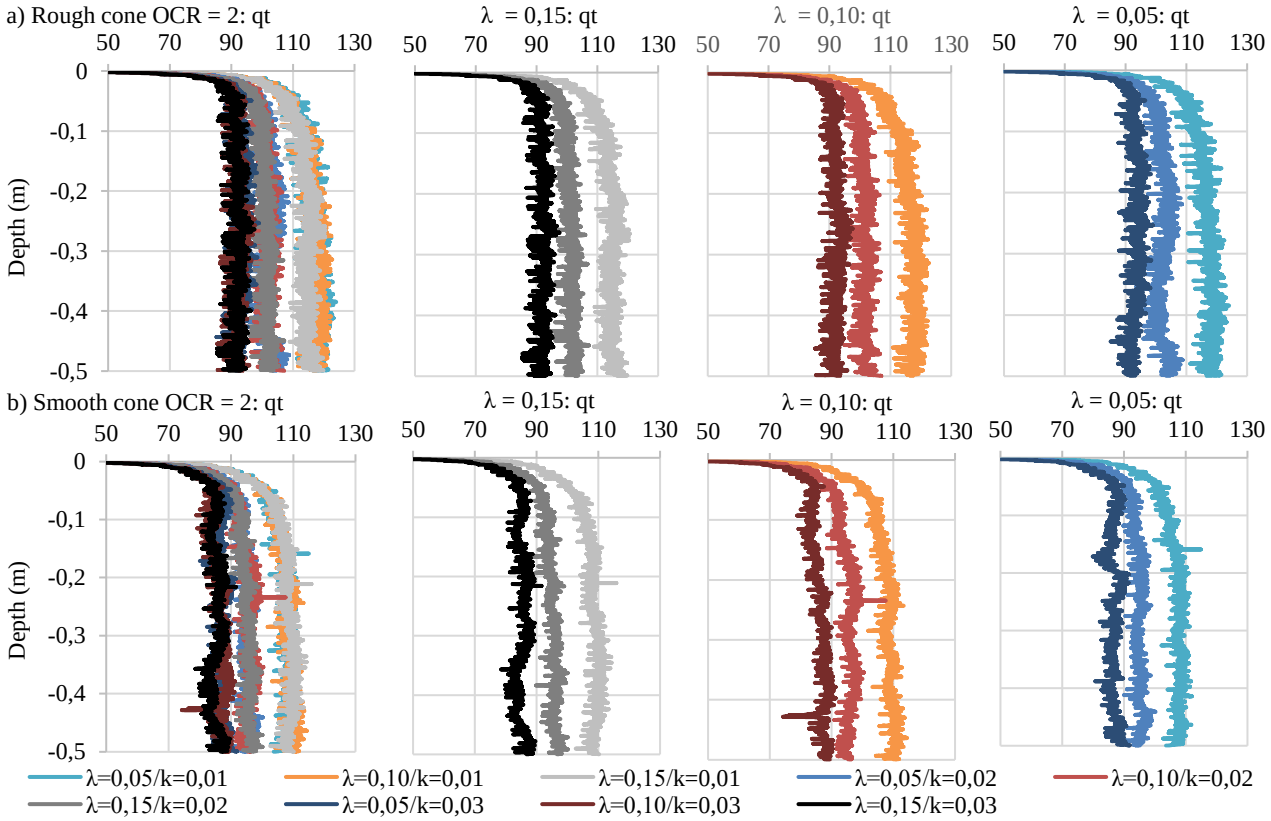

Figure 10. The influence of the compressibility parameters λ and κ in the tip resistance (q_t) for the OCR = 2

generate a considerable negative porewater pressure and p > q > u, while in Fig. 4 q > p > u, indicating that after the cone passes, the shear forces are predominant, following Robertson *et al.* (1986).

Regarding Pocket G-PFEM performance, in Fig. 7, q_t, u_1 and u_2 profiles reach a steady state condition after 0.05 m deep, but the f_s and u_3 profiles only reach constant values after 0.20 m deep. The delay between the measurements is associated with the fact that at the begin-

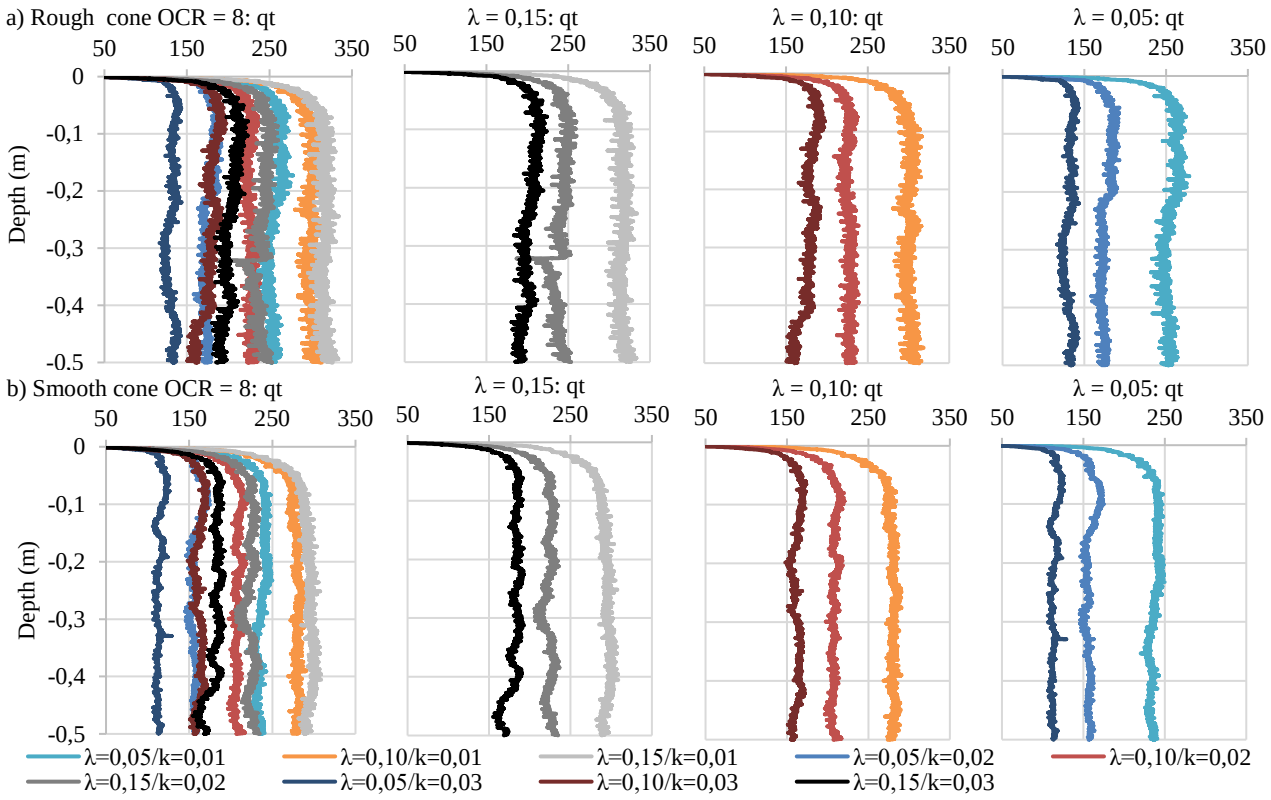

Figure 11. The influence of the compressibility parameters λ and κ in the tip resistance (q_t) for the OCR = 8.

-ning of the calculation, the fs measurement position is partially inserted in the soil, and the u3 position is not yet inserted, resulting in more time for fs and u3 to reach a steady state. Compared to the results presented by Song et al. (2019), the Pocket G-PFEM reached a steady state condition 2.5 to 10 times faster.

5.2. Influence of compressibility

The compressibility effect on q_t is presented for OCR equals 1, 2 and 8 in Fig. 9, Fig. 10, and Fig. 11, respectively. Fig.9 shows that the tip resistance is mainly affected by λ for the OCR =1. The higher the λ, the lower the q_t. It is interesting to notice that for λ = 0.05, the q_t is not significantly affected by the variation of κ. However, for λ = 0.10 and λ = 0.15, higher κ results in slightly lower cone tip resistance. Looking at CASM formulation, it is expected q_t in normally consolidated soils (OCR = 1) to be influenced by λ and κ because in this state, any increase in the mean and deviatoric stresses results in plastic strains governed by a strain-hardening rule (Eq. 5) dependent on both parameters (Mánica *et al.*, 2022). The little change in q_t for λ = 0.05 when changing κ may be related to the magnitude of the adopted values.

$$\frac{dp'_0}{d\varepsilon_v^p} = \frac{p'_0 v_0}{\lambda - \kappa} \quad (5)$$

Where, $d\varepsilon^p_v$ is the volumetric plastic strain increment resultant of the mean stress increment dp'_0, and v_0 is the initial specific volume.

For the OCR = 2, presented in Fig. 10, the tip resistance is only affected by the swelling index. The higher the κ, the lower the q_t. The simulations did not show any influence of λ in the cone tip resistance, and q_t was the same for the three tested λ values. It indicates that the q_t is mainly associated with elastic strains for the OCR = 2, and the computed stresses are still inside the yield surface.

For the OCR = 8, presented in Fig. 11, the tip resistance is considerably affected by the swelling index, and the higher the κ, the lower the q_t. Differently from the results obtained for the OCR = 2, the q_t is also affected by the compressibility index for the OCR = 8. For this overconsolidation ratio, the value of the tip resistance increases with the increase of λ. Thus, a more compressible soil tends to show higher q_t, which is not consistent with the behaviour described by Robertson & Campanella (1983), Jamiolkowski *et al.* (1985), Lunne *et al.* (1997), Robertson (2009), Jefferies & Been (2016).

Two different behaviours are observed depending on how overconsolidated the material is. By increasing the OCR, it was expected that the strains would be even more in the elastic domain so that they would be even more dependent on κ. However, the identified limitation corresponds to the expected behaviour for the Modified Cam-Clay model mimicked by the adopted CASM parameters. The MCC overestimate the dilation of overconsolidated soils (Carneiro et al. 2023). Higher λ results in more post-yield plastic deformation and higher undrained strength (higher q_t), as illustrated by the undrained triaxial compression simulation in Fig. 12.

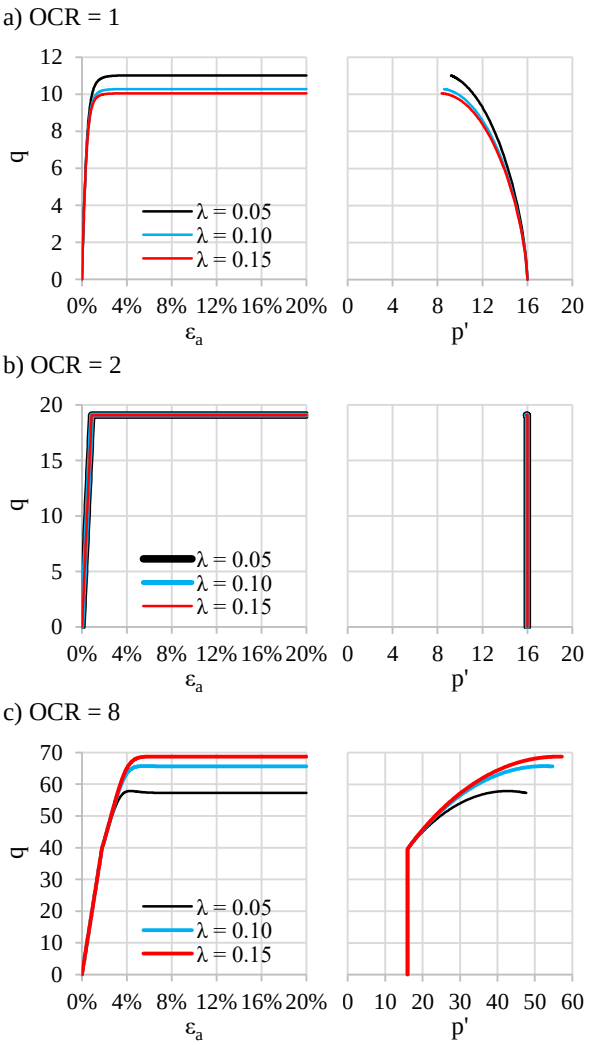

Figure 12. Stress-strain responses in an undrained triaxial compression simulation in the element testing widget (CIMNE 2023) with the parameters adopted in this study (MCC mimicked by CASM). The swelling slope was kept constant (κ = 0.05). a) OCR = 1, b) OCR = 2, and c) OCR =8.

Lastly, comparing the results of the rough and smooth cones, the q_t obtained with the rough cone was always slightly higher than the one registered with the smooth cone for all combinations of λ and κ.

6. Conclusions

Being able to simulate a CPTu is a considerable advance in geotechnical engineering. The Pocket G-PFEM is a powerful tool to be used in the future. With rapid analysis response, the Pocket G-FEM could be used to evaluate different scenarios in homogeneous strata, allowing the optimization of investigation campaigns and prediction of changes in the soil layer behaviour due to changes in the boundary conditions.

This study shows Pocket G-PFEM limitations to reproducing the sleeve friction and porewater pressure

generation in the u_2 and u_3 positions. It also highlights well-known limitations of the Modified Cam-Clay, mimicked by the adopted CASM parameters; the analyses with higher compressibility index resulted in higher cone tip resistances for the OCR = 8.

As some of the limitations are associated with the adopted parameters, it is recommended that similar analyses with different parameters should be performed to evaluate the software's performance. Future studies should also include:

- Evaluation of the effect of the hydraulic conductivity on the results.
- Evaluation of the effect of the cone penetration speed on the results.
- Comparison of the Pocket G-PFEM results with the results of real CPTu performed in homogeneous layers.

Acknowledgements

The authors would like to acknowledge the support received by Pimenta de Ávila Consultoria and the Universitat Politècnica de Catalunya for the paper development.

References

Carneiro, J., Faria, A., and Junior, M. "Calibration of Modified Cam-Clay Parameters for Red Mud Tailings – A Case Study", In: Tailings and Mine Waste 2023, Vancouver, Canada, 2023, pp. 69-80.

CIMNE, and Universitat Politècnica de Catalunya, "Pocket G-PFEM - User Manual", 2nd ed., Catalunya, Spain, 2023, pp. 1-28.

Hauser, L., and Schweiger, H.F., "Numerical study on undrained cone penetration in structured soil using G-PFEM", Computers and Geotechnics 133, no. 104061, 2021. https://doi.org/10.1016/j.compgeo.2021.104061

Jamilkowski, M., C. C. Ladd, J. T. Germaine, and R. Lancellotta. "New developments in field and laboratory testing of soils", In: 11th International Conference on Soil Mechanics and Foundation Engineering, San Francisco, USA, 1985, pp. 57-154.

Jefferies, M., and K. Been. "Soil Liquefaction: A Critical State Approach", 2nd ed., CRC Press, Boca Raton, USA, 2016.

Lunne, T., P. K. Robertson, and J. J. M. Powell. "Cone Penetration Testing in Geotechnical Practice", 1st ed., CRC Press, 1997.

Mánica, M. A., Arroyo, M., Gens, A., & Monforte, L. "Application of a critical state model to the Merriespruit tailings dam failure", In: Proceedings of the Institution of Civil Engineers: Geotechnical Engineering, 175(2), pp. 151-165, 2022. https://doi.org/10.1680/jgeen.21.00001

Mayne, P. W. "Stress-strain-strength-flow parameters from enhanced in-situ tests", In: International Conference on In Situ Measurement of Soil Properties and Case Histories, Bali, Indonesia, 2001, pp. 27-47.

Robertson, P. K., and R. G. Campanella. "Interpretation of cone penetration tests. Part I: Sand", Canadian Geotechnical Journal, 20 (4), pp. 718-733, 1983.

Robertson, P. K., R.G. Campanella, D. Gillespie, and J. Greig. "Use of piezometer cone data", In: Use of In-situ Testing in Geotechnical Engineering, Blacksburg, USA, 1986, pp. 1263-1280.

Robertson, P. K. "Interpretation of cone penetration tests – a unified approach", Canadian Geotechnical Journal, 46, pp. 1337-1355, 2009. https://doi.org/10.1139/T09-065

Roy, M., Tremblay, F. Tavenas, and P. F. & La Rochelle, "Development of porewater pressure in quasi-static penetration tests in sensitive clay", Canadian Geotechnical Journal, 19 (2), pp. 124-138, 1982. https://doi.org/10.1139/t82-015

Song, C., B. Bekele, and A. Silvey. "Porewater pressure responses of Overconsolidated Soils in a Partially Drained Piezocone Penetration Test", Journal of Engineering Mechanics, 145(4), pp. 1-10, 2019. https://doi.org/10.1061/(ASCE)EM.1943-7889.0001594

Yu, H. S. "CASM: a unified state parameter model for clay and sand", International Journal for Numerical and Analytical Methods in Geomechanics, 22, pp. 621-653, 1998. https://doi.org/10.1002/(SICI)1096-9853(199808)22:8<621::AID-NAG937>3.0.CO;2-8